1-1-2015

A practical path planning methodology for wire and arc additive manufacturing of thin-walled structures

Donghong Ding
University of Wollongong, dd443@uowmail.edu.au

Zengxi Pan
University of Wollongong, zengxi@uow.edu.au

Dominic Cuiuri
University of Wollongong, dominic@uow.edu.au

Huijun Li
University of Wollongong, huijun@uow.edu.au

A practical path planning methodology for wire and arc additive manufacturing of thin-walled structures

Abstract

This paper presents a novel methodology to generate deposition paths for wire and arc additive manufacturing (WAAM). The medial axis transformation (MAT), which represents the skeleton of a given geometry, is firstly extracted to understand the geometry. Then a deposition path that is based on the MAT is efficiently generated. The resulting MAT-based path is able to entirely fill any given cross-sectional geometry without gaps. With the variation of step-over distance, material efficiency alters accordingly for both solid and thin-walled structures. It is found that thin-walled structures are more sensitive to step-over distance in terms of material efficiency. The optimal step-over distance corresponding to the maximum material efficiency can be achieved for various geometries, allowing the optimization of the deposition parameters. Five case studies of complex models including solid and thin-walled structures are used to test the developed methodology. Experimental comparison between the proposed MAT-based path patterns and the traditional contour path patterns demonstrate significant improved performance in terms of gap-free cross-sections. The proposed path planning strategy is shown to be particularly beneficial for WAAM of thin-walled structures.

Keywords

walled, thin, manufacturing, additive, arc, wire, structures, methodology, practical, planning, path

Disciplines

Engineering | Science and Technology Studies

Publication Details

Ding, D., Pan, Z., Cuiuri, D. & Li, H. (2015). A practical path planning methodology for wire and arc additive manufacturing of thin-walled structures. Robotics and Computer Integrated Manufacturing, 34 8-19.

A practical path planning methodology for wire and arc additive manufacturing of thin-walled structures

Donghong Ding, Zengxi Pan*, Dominic Cuiuri, Huijun Li

School of Mechanical, Materials, and Mechatronics Engineering, Faculty of Engineering and Information Sciences, University of Wollongong, Northfield Ave, Wollongong, NSW 2500, Australia

Abstract: This paper presents a novel methodology to generate deposition paths for wire and arc additive manufacturing (WAAM). The medial axis transformation (MAT), which represents the skeleton of a given geometry, is firstly extracted to understand the geometry. Then a deposition path that is based on the MAT is efficiently generated. The resulting MAT-based path is able to entirely fill any given cross-sectional geometry without gaps. With the variation of step-over distance, material efficiency alters accordingly for both solid and thin-walled structures. It is found that thin-walled structures are more sensitive to step-over distance in terms of material efficiency. The optimal step-over distance corresponding to the maximum material efficiency can be achieved for various geometries, allowing the optimization of the deposition parameters. Five case studies of complex models including solid and thin-walled structures are used to test the developed methodology. Experimental comparison between the proposed MAT-based path patterns and the traditional contour path patterns demonstrate significant improved performance in terms of gap-free cross-sections. The proposed path planning strategy is shown to be particularly beneficial for WAAM of thin-walled structures.

Keywords: path planning, additive manufacturing, medial axis transformation, thin-walled, material efficiency

1. Introduction

Additive manufacturing (AM) or 3D printing, which is based on layer-by-layer manufacturing approach instead of conventional material removal methods, has gained worldwide popularity over the past thirty years [1]. The original techniques include stereolithography apparatus [2], laminated object manufacturing [3], fused deposition modelling [4], 3D printing [5] and selective laser sintering [6]. These AM processes are typically applied to fabricate polymer parts which are usually used for prototyping or illustrative purposes. The current development focus of AM has shifted to producing functional metal components of complex shape that can meet the demanding requirements of the aerospace, defence, and automotive industries [7]. Wire and arc additive manufacturing (WAAM) is by definition an arc-based process that uses either the gas tungsten arc welding (GTAW) or the gas metal arc welding (GMAW) process has drawn the interest of the research community in recent years due to its high deposition rate [8-10]. This technique has

been presented to the aerospace manufacturing industry as a unique low cost solution for manufacturing large thin-walled structures through significantly reducing both product development time and "buy-to-fly" ratios [11-12].

One of the crucial tasks in WAAM is the generation of paths which guide the motion of the deposition head to fill the 2D layers representing the cross-sectional geometry of an object. Many types of path patterns have been developed for AM, as summarized in Table 1 [13-26]. It is found that the essential step to generate paths is offsetting. Commonly used patterns are raster patterns which offset parallel to a given direction, and contour patterns which offset parallel to the boundary of geometry. Other path patterns are either variations or combinations from these general strategies.

Contour path patterns are often preferred over raster path patterns for producing thin-walled metal structures due to certain practical concerns. Raster path patterns build the whole component along the same direction, which means the deposition head is required to be turned frequently, leading to a poor building quality [26]. In addition, the fabricated component will have warpage and anisotropic problems. By following the boundary trend of the geometry, the contour path method overcomes the warpage as well as anisotropic issues by changing path direction constantly along the boundary curves of the sliced layer [26].

However, the contour path patterns pose a severe quality problem of potentially leaving gaps within the deposited layers. This is because the contour paths, which are generated by offsetting the boundary curves recursively toward its interior, do not guarantee to completely fill a desired 2D geometry. As shown in Fig.1, a cross-section of a simple thin-walled geometry is described by the boundary (Fig.1a). The contour paths (green lines shown in Fig.1b) are generated by offsetting the boundary towards its interior with the i^{th} contour path offset at distance $(i-\frac{1}{2})d$ from the boundary, where d is the step-over distance. The step-over distance is defined as the distance between the next deposition track and the previous one. For WAAM, the overlapping of weld beads is necessary to achieve smooth surface. As shown in Fig.2, weld beads are overlapped with the certain step-over distance (centre distance d). According to different weld bead overlapping model, the optimal step-over distance d is the function of weld bead width w , which $d = 0.667\ w$, or $d = 0.738\ w$ [27]. The deposition process can be considered as a constant-radius disk with the diameter of d being swept along the computed path. It is found that contour path patterns leave narrow gaps since there is not enough space for offsetting the next path as the middle white area shown in Fig.1c. The area of the produced gaps is highly dependent on the step-over distance d, which varies for different AM system. For powder-based AM, d could be generally small within the range of 0.01 mm to 1 mm. The negative effects of gaps with small area on the quality of the produced components could be neglected for many applications. However, for WAAM d typically varies from 2 mm to 12 mm depending on the diameter of the feed wire, the travel speed of deposition head, and the wire feed rate. Gaps resulting from poorly planned paths in WAAM could be a severe problem, especially for thin-walled structures. The unavoidable gaps may potentially lead to structural failure of highly loaded components.

Possible solutions to the gap problem can be reducing the step-over distances or revisiting the gaps through overlapping the deposition path. However, as has been mentioned, the step-

over distance is limited by the deposition system, and will affect the deposition rate. Moreover, the work pieces may have a complex structure where wall thickness varies along its boundary, making it impossible to fill the entirely region using contour path patterns. On the other hand, the strategy of revisiting requires the deposition head to move into a small unfilled region that is surrounded by deposited material. Voids or gaps are often produced during such “infilling” due to the difficulty for material to fully reach into the confined corners of an unfilled region.

Kao [28] has proposed an alternative methodology of using the Medial Axis Transformation (MAT) of the geometry to generate the offset curves by starting at the inside and working towards the outside, instead of starting from the boundary and filling towards the inside. This approach is able to compute paths which can entirely fill the interior region of geometry as the paths are generated from interior to the boundary. This strategy avoids producing gaps by depositing excess material outside the boundary, as illustrated in Fig. 3. The extra material can subsequently be removed by post-processing. Therefore, the traditional contour path patterns from outside to inside is natural for machining whereas MAT-based path starting from inside and working towards the outside is suitable for WAAM of void-free components. However, the authors limit their discussion to geometries with simple MAT paths, and the MAT-based path for general geometries or arbitrary shapes, to our knowledge, is still unavailable.

This study presents a methodology of generating MAT-based paths for an arbitrary geometry, either thin-walled or solid structures, with or without internal holes. Gap-free paths are successfully obtained using the proposed approach. Furthermore, the optimal step-over distance corresponding to the maximum material efficiency is discussed for various geometries. It is found that the proposed path planning methodology is particularly beneficial to WAAM of thin-walled structures. After this introductory section, section 2 presents the Medial Axis Transform (MAT) and its computing algorithms. Section 3 introduces the methods for generating paths from MAT, followed by the implementation and the discussions of the proposed methodology in Section 4. The paper ends with the conclusions in Section 5.

2. Medial axis transformation (MAT)

2.1 Definition

The Medial Axis Transformation (MAT) is a technique first proposed by Blum [29] to describe shapes with the medial axis which is defined as loci of centres of locally maximal balls inside an object. In two dimensions, as shown in Fig.4, the MAT would be the loci of centres of locally maximal disks inside the region. The points on the medial axis are called medial axis points as represented by the dash line. The medial axis points are further classified into end points, normal points, and branch points depending on the number of points where the disk touches the boundary [28]. If the disk touches the boundary at either two connected segments, two points, or one segment and one point, the medial axis point is a normal point. For those disks touching the boundary at more than two points or connected segments, such medial axis points are branch points. The remaining medial axis points are end points which are also the vertices of the geometry.

The medial axis of geometry is also called the skeleton because of its shape. Associated with the medial axis is a radius function, which defines for each point on the axis its distance to the boundary of the geometry. The medial axis and the radius function together are important topological information of the given geometry, allowing the later path planning to be performed in a more efficient and convenient manner.

2.2 Method to compute the MAT

Medial Axis Transformation, or skeletonization, has been widely studied over the past few decades in the computer vision field. Lee [30] proposed a divide-and-conquer approach that constructs the generalized Voronoi diagram for simple polygons. The medial axis transformation can be easily extracted by removing the Voronoi edges connecting to concave vertices of the polygon. Srinivasan et al. [31] extends Lee's algorithm to computing a generalized Voronoi diagram for polygons with holes. Choi [32] presents an MAT approximation algorithm in the planar domain via domain decomposition. Kao [34] proposes a method that directly associates boundary points to the corresponding proximity metrics based on Lee's and Srinivisan's methodology.

Based on Lee's and Kao's approach, a simple MAT method is developed through computing the bisector of each pair of segments. As shown in Fig.5, the geometry is represented by line segments *ab*, *bc*, *cd*, *de*, and *ea*. For line segment *ab*, there are four pairs, and the bisectors of each pairs, *B(ab, bc), B(ab, cd), B(ab, de), B(ab, ea),* are computed. Each bisector of two closed line segments (a pair) is formed by straight lines and parabolic curves as shown in Fig. 5a. By definition, the MAT produces a set of lines which divide the geometry into several sub-regions. In each sub-region, all the points are closet to its associated boundary. Therefore, the medial axis is constructed by using the bisectors which are closest to the relevant boundary, as the bold red line shown in Fig. 5b. The detailed computing algorithms can be found in the literature [30-33].

3. MAT Path planning methodology

The overview of the developed algorithms is described as shown in Fig. 6. The flowchart of the algorithms consists of two phases: *Phase 1*, preparing the MAT of the geometry; and *Phase 2*, generating the path from the medial axis. The MATs for various geometries are successfully computed as shown in Fig. 7-9 (a). Algorithms for phase 1 (from CAD model to MAT) are not detailed in this study since they have been reported elsewhere in the literature [33, 34]. The detailed algorithms for *Phase 2* are presented in this section.

This study classifies the MAT into branches and sub-branches. Branches are the line segments consisting of the MAT points between two branch points, while sub-branches are line segments consisting of the MAT points between one branch point and one end point. Those branches are extracted by *Extract branches* module, as shown in Fig. 7-9 (b).

Extracted branches are formed to various branch loops. Depending on the shape of the geometry, three possible situations have been found. For geometry with a single branch, a single branch loop is formed along the counter-clockwise direction as shown in Fig. 7c. For geometry with multiple branches without holes, a single branch loop is formed along the counter-clockwise direction as well shown in Fig. 8c. Lastly, for geometry with holes, several

branch loops would be formed according to the number of holes. Among them, the branch loop is in the contour-clockwise direction corresponding to the outside boundary of the geometry, while other loops are in the clockwise direction corresponding to the inside hole boundaries, as shown in Fig. 9c. Branch loops are stored in the format of Branch_loops { *j* }, where *j* represents the number of loops.

Paths are generated by recursively offsetting contour-clockwise branch outward and clockwise branches inward at distance $(i-\frac{1}{2})d$. *i* represents i^{th} offset, and *d* represents the step-over distance. It should be noted that during the offsetting self-intersection may happen regardless of whether it is inward or outward offset. Algorithm for solving self-intersection is not detailed in this paper since they have been reported elsewhere in the literature [17]. As shown in Fig.6, Path { *i, j* } represents the i^{th} offset of the Branch_loops { *j* }. Path_B { *i, j* } represents the path outside boundary of the i^{th} path. When the area of the i^{th} path boundary *j* is larger than its relevant contour { *j* }, and there is no intersection between the boundary and the contour, the Branch_loops { *j* } will be updated to empty. Meanwhile the offsetting of this branch loop will be ceased since the region relevant to this branch loop is fully filled by deposition material. The iterative procedure ends when all the branch loops are updated to be empty and there is no more offset needed. The output is a set of untrimmed paths, and the structures of the untrimmed paths for the geometry in Fig.9 are shown in Fig. 10 using Matlab cell structures. There are three branch loops corresponding to three columns in Fig. 10, and the iterative procedure ceases at the 6^{th} offset. The generated untrimmed paths for the geometry in Fig. 7 are shown in Fig. 11 (a). The whole procedure ceases after the 5^{th} offset as the area of the 5^{th} path boundary (the outside blue lines) is larger than the area of the geometry and there is no intersection between them. It can be seen from Fig.11 (a) that the geometry is fully filled but there is an obvious excess of deposited material. To improve the material efficiency, the last step is to trim the paths. The parts of blue lines outside of the geometry represent extra materials and the associated paths are trimmed as shown in Fig. 11 (b).

Using the MAT-based path generated in this study, the gaps that would be generated by using traditional contour path patterns are removed. However, this has been achieved at the cost of creating some discontinuity of the path and extra deposition at the boundary. Post-processing, such as milling or grinding, is required to remove excess materials and improve the accuracy of the fabricated components. Material efficiency, which defined as the ratio of the real area of the geometry to the deposited area, is an important factor for the AM process. Material efficiency, *E*, is expressed as: $E = A_r/A_d = A/(Ld)$. A_r represents the real area of the geometry; A_d represents the deposited material which is calculated by times of the total path length *L* and the step-over distance *d*. Material efficiency at various step-over distances will be discussed in the next section.

4. Implementation and discussions

Five geometries sliced from CAD models are tested to validate the effectiveness and robustness of the developed algorithms. As shown in Fig. 12-16, various types of geometries

are tested including solid structures with or without holes, and thin-walled structures. Table 2 provides basic information of the geometries. The MATs and the trimmed paths for all geometries are successfully generated using the developed algorithms.

The material efficiency of AM, based on the proposed MAT-based path at various step-over distances, is simulated for the different geometries as shown in Fig.17. Material efficiency of the traditional CNC machining is also provided as a comparison. It is found that, in general, material efficiency decreases with the increasing of step-over distance. This is intuitive as step-over distance represents the resolution of the deposition system. To fill geometry with deposition material, the greater the step-over distance, the more excess material will need to be deposited. The results also show that AM technology has a much higher material efficiency compared to traditional subtractive manufacturing.

The effects of the step-over distance on part building time are also discussed. The building time t is determined by the sum of the total path length L and the travel speed, V, of the deposition head. If the build time at the step-over distance of 1 mm, t_1, is set to be the characteristic time, the non-dimensional building time T at the step-over distance of d is expressed as $T = \frac{t_d}{t_1} = \frac{L_d / V}{L_1 / V} = \frac{L_d}{L_1}$. Where, L_d represents the total path length at the step-over distance of d; and the travel speed V is assumed to be the same at various step-over distances. The non-dimensional building time as the function of step-over distances are calculated as shown in Fig.17. With the increasing of the step-over distance, the build time T declines exponentially. It reveals that it is always better to have a small step-over distance for high material efficiency whereas that would be at the expense of productivity.

For powder-based AM system, the step-over distance generally ranges from 0.01mm to 2 mm. Material efficiency in this range decreases only slightly, indicating that the step-over distance does not have a significant effect on the material efficiency of powder-based AM. As inferred above, material efficiency is determined by the resolution of the deposition system in relation to the size of the geometry. Building time changes significantly in this range, therefore, build rate will be an important factor for powder-based AM system.

On the other hand, for WAAM technology, the typical step-over distance varies from 2 mm to 12 mm for mild steel materials. Building time in this range as shown in Fig.17 doesn't change significantly and therefore build rate for WAAM is not the major concern. Material efficiency in WAAM using the proposed MAT-based paths is shown in Fig. 18. It is found that for solid structures (Geometry 1 and Geometry 2) material efficiency is relatively constant, with a slight decrease as step-over distance increases. However for thin-walled structures, such as Geometry 3, 4, and 5, the variation of material efficiency corresponding to the step-over distance are significant. Although the generally-descending trend of material efficiency can still be found, the variation cannot be predicted since the shapes of various geometries are very different. The optimal step-over distances for Geometry 1 and 2 are 4 mm, while for Geometry 3 is around 4 mm, for Geometry 4 is near 6 mm and for Geometry 5 is approximately 3 mm.

Variations of material efficiency in WAAM for the five tested geometries are shown in Fig. 19. It is clear that while the variation of material efficiency for different step-over distances is minimal for solid structures, it is quite significant for thin-walled structures. For

geometry 5, by choosing the optimal step-over distance, material efficiency could be increased by 2.4 times from 38.63% to 94.15%. This indicates that step-over distance plays an important role on material efficiency when fabricating thin-walled structures using WAAM technology.

Experimental results of the proposed MAT-based path generation strategy are conducted using a robotic welding system at the University of Wollongong as shown schematically in Fig. 20. The details of the system can be found in previous publications [36]. In this study, a section of Geometry 5 is fabricated using both the proposed MAT-based path patterns and the traditional contour path patterns.

Comparisons between the proposed path patterns and the traditional contour path patterns are shown in Fig. 21. For the proposed path patterns (Fig. 21a), layers are generated by offsetting the deposition head from the medial axis to outside, and the deposited layers are slightly larger than real geometry. For the traditional path patterns (Fig. 21b), deposited layers are consistent to the real geometry boundaries; however, gaps are created since the thicknesses of the walls vary. After surface milling, it can be seen that, while the traditional contour path patterns (Fig. 21d) leaves gaps on the component, the proposed MAT-based path patterns are able to produce gap-free walls. Depending on the thickness of the walls, more material may need to be removed for the parts generated using the proposed MAT-based path patterns, in order to produce the desired geometry. However, for certain applications such as AM components subjected to high mechanical loading, the extra material removal is less of an issue than leaving gaps in the interior of the deposited parts using traditional contour path patterns.

5. Conclusions

This paper presents a novel methodology of path planning for the additive manufacturing process. Gap-free paths can be achieved using the proposed algorithm through offsetting the medial axis of the given geometry towards its boundary. This gap-free path improves the quality of the fabricated components partially for thin-walled structures. The developed algorithms and methodology are demonstrated to be effective and robust for arbitrarily shaped geometries through testing five complex samples.

Material efficiency in relation to different step-over distances is discussed in details. While there is minimal effect of step-over distance on material efficiency for powder-based AM technology, the effects of step-over distance on material efficiency are significant for WAAM technology due to the high deposition rate and the relatively large step-over distance. Material efficiency is found to be particularly sensitive to step-over distance vary for thin-walled structures. With an appropriate step-over distance, material efficiency can be more than doubled for some thin-walled structures.

Experiments have demonstrated that improved part quality is achieved by using the proposed MAT-based path patterns in comparison to the traditional contour path patterns. The proposed path planning is able to produce completely gap-free component, which is not possible using previous path generation strategies. As a result, the MAT-based path planning strategy should be particularly beneficial for WAAM of thin-walled structures in terms of both improved quality and material efficiency.

Acknowledgements

This work was supported by the Defence Materials Technology Centre (DMTC), which was established and is supported by the Australia Government's Defence Future Capability Technology Centre (DFCTC) initiative. The authors would like to thank Professor J. Norrish for his expertise in the welding field. N. Larkin is especially thanked for his assistance with the experiments. This work is supported in part by the State Scholarship Fund of the China Scholarship Council (No. 2011684067).

References

[1] G.N. Levy, R. Schindel, J.P. Kruth, Rapid manufacturing and rapid tooling with layer manufacturing (LM) technologies, state of the art and future perspectives, CIRP Annals-Manufacturing Technology, vol. 52, pp. 589-609, 2003.

[2] X. Yan, P. Gu, A review of rapid prototyping technologies and systems, Computer-Adied Design, vol. 28, pp. 307-318, 1996.

[3] M.J. Tari, A. Bals, J. Park, M.Y. Lin, H.T. Hahn, Rapid prototyping of composite parts using resin transfer molding and laminated object manufacturing. Composites Part A: Applied Science and Manufacturing, vol. 29, pp. 651-661, 1998.

[4] I. Zein, D.W. Hutmacher, K.C. Tan, S.H. Teoh, Fused deposition modeling of novel scaffold architectures for tissue engineering applications, Biomaterials, vol. 23, pp. 1169-1185, 2002.

[5] E. Sachs, et al., Three-Dimensional Printing: Rapid Tooling and Prototypes Directly from a CAD Model, CIRP Annals - Manufacturing Technology, vol. 39, pp. 201-204, 1990.

[6] M. Agarwala, D. Bourell, J. Beaman, H. Marcus, J. Barlow, Direct selective laser sintering of metals. Rapid Prototyping Journal, vol. 1, pp. 26-36.

[7] D. Gu, et al., Laser additive manufacturing of metallic components: materials, processes and mechanisms, International materials reviews, vol. 57, pp. 133-164, 2012.

[8] J. Xiong, et al., Vision-sensing and bead width control of a single-bead multi-layer part: material and energy savings in GMAW-based rapid manufacturing, Journal of Cleaner Production, vol. 41, pp. 82-88, 2013.

[9] J. Xiong, et al., Modeling of bead section profile and overlapping beads with experimental validation for robotic GMAW-based rapid manufacturing, Robotics and Computer-Integrated Manufacturing, vol. 29, pp. 417-423, 2013.

[10] K. Karunakaran, et al., Low cost integration of additive and subtractive processes for hybrid layered manufacturing, Robotics and Computer-Integrated Manufacturing, vol. 26, pp. 490-499, 2010.

[11] P. S. Almeida and S. Williams, Innovative process model of Ti–6Al–4V additive layer manufacturing using cold metal transfer (CMT), in Proceedings of the Twenty-first Annual International Solid Freeform Fabrication Symposium, University of Texas at Austin, Austin, TX, USA, 2010.

[12] P. A. Colegrove, et al., Microstructure and residual stress improvement in wire and arc additively manufactured parts through high-pressure rolling, Journal of Materials Processing Technology, vol. 213, pp. 1782-1791, 2013.

[13] M. R. Dunlavey, Efficient polygon-filling algorithms for raster displays, ACM Transactions on Graphics (TOG), vol. 2, pp. 264-273, 1983.

[14] S. C. Park and B. K. Choi, Tool-path planning for direction-parallel area milling, Computer-Aided Design, vol. 32, pp. 17-25, 2000.

[15] V. Rajan, et al., The optimal zigzag direction for filling a two-dimensional region, Rapid Prototyping Journal, vol. 7, pp. 231-241, 2001.

[16] R. Farouki, et al., Path planning with offset curves for layered fabrication processes, Journal of Manufacturing Systems, vol. 14, pp. 355-368, 1995.

[17] Y. Yang, et al., Equidistant path generation for improving scanning efficiency in layered manufacturing, Rapid Prototyping Journal, vol. 8, pp. 30-37, 2002.
[18] H. Li, et al., Optimal toolpath pattern identification for single island, sculptured part rough machining using fuzzy pattern analysis, Computer-Aided Design, vol. 26, pp. 787-795, 1994.
[19] H. Wang, et al., A metric-based approach to two-dimensional (2D) tool-path optimization for high-speed machining, Transanctions-American Society of Mechanical Engineers Journal of Manufacturing Science and Engineering, vol. 127, p. 33-48, 2005.
[20] F. Ren, et al., Combined reparameterization-based spiral toolpath generation for five-axis sculptured surface machining, The international journal of advanced manufacturing technology, vol. 40, pp. 760-768, 2009.
[21] M. Bertoldi, et al., Domain decomposition and space filling curves in toolpath planning and generation, in Proceedings of the 1998 Solid Freeform Fabrication Symposium, The University of Texas at Austin, Austin, Texas, 1998, pp. 267-74.
[22] T. Wasser, et al., Implementation and evaluation of novel buildstyles in fused deposition modeling (FDM), Strain, vol. 5, pp. 95-102, 1999.
[23] R. Dwivedi and R. Kovacevic, Automated torch path planning using polygon subdivision for solid freeform fabrication based on welding, Journal of Manufacturing Systems, vol. 23, pp. 278-291, 2004.
[24] D. Ding, Z. Pan, D. Cuiuri, H. Li, A tool-path generation strategy for wire and arc additive manufacturing, The international journal of advanced manufacturing technology, vol. 73, pp. 173-183, 2014.
[25] Y. Zhang, et al., Weld deposition-based rapid prototyping: a preliminary study, Journal of Materials Processing Technology, vol. 135, pp. 347-357, 2003.
[26] G. Jin, et al., An adaptive process planning approach of rapid prototyping and manufacturing, Robotics and Computer-Integrated Manufacturing, vol. 29, pp. 23-38, 2013.
[27] D. Ding, Z. Pan, D. Cuiuri, H. Li, A multi-bead overlapping model for robotic wire and arc additive manufacturing, Robotics and Computer-Integrated Manufacturing, vol. 31, pp. 101-110, 2015.
[28] J.-H. Kao and F. B. Prinz, Optimal motion planning for deposition in layered manufacturing, in Proceedings of DETC, 1998, pp. 13-16.
[29] H. Blum, A transformation for extracting new descriptors of shape, Models for the perception of speech and visual form, vol. 19, pp. 362-380, 1967.
[30] D.-T. Lee, Medial axis transformation of a planar shape, Pattern Analysis and Machine Intelligence, IEEE Transactions on, pp. 363-369, 1982.
[31] V. Srinivasan and L. R. Nackman, Voronoi diagram for multiply-connected polygonal domains 1: algorithm, IBM Journal of Research and Development, vol. 31, pp. 361-372, 1987.
[32] H. I. Choi, et al., New algorithm for medial axis transform of plane domain, Graphical Models and Image Processing, vol. 59, pp. 463-483, 1997.
[33] J.-H. Kao, Process planning for additive/subtractive solid freeform fabrication using medial axis transform, Citeseer, 1999.
[34] S. Choi, K. Kwok, A tolerant slicing algorithm for layered manufacturing, Rapid Prototyping Journal, vol. 8, pp. 161-179, 2002.

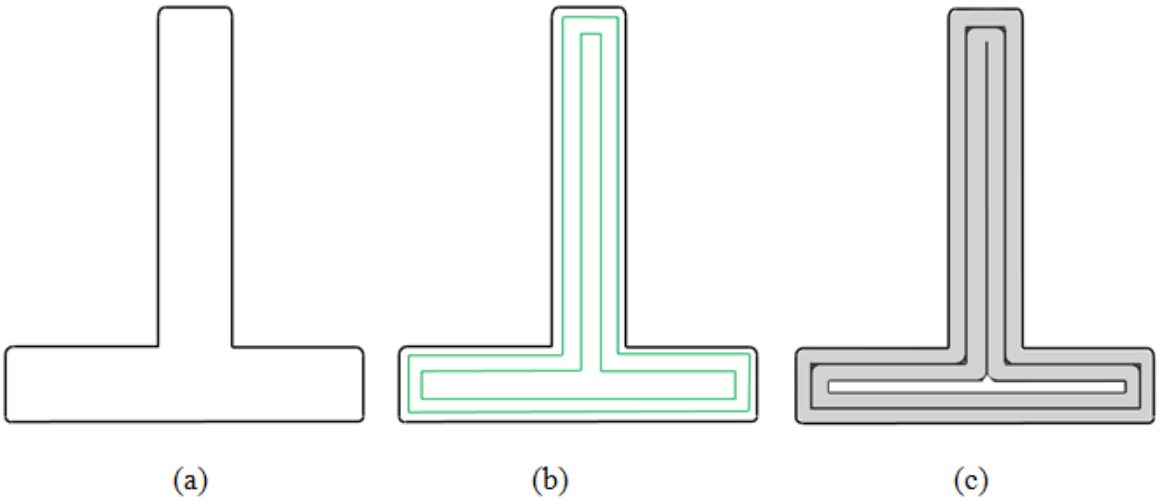

Fig.1 (a) A cross-section of a simple thin-walled structure. (b) Contour path patterns generated by offsetting the boundary curves towards its interior. (c) Deposition of materials along the generated path. Narrow gap (middle white area) is left which cannot be filled by the path.

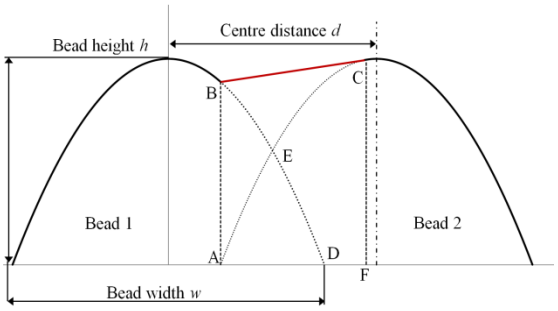

Fig.2 Illustrations of step-over distance (or centre distance *d*) [27]

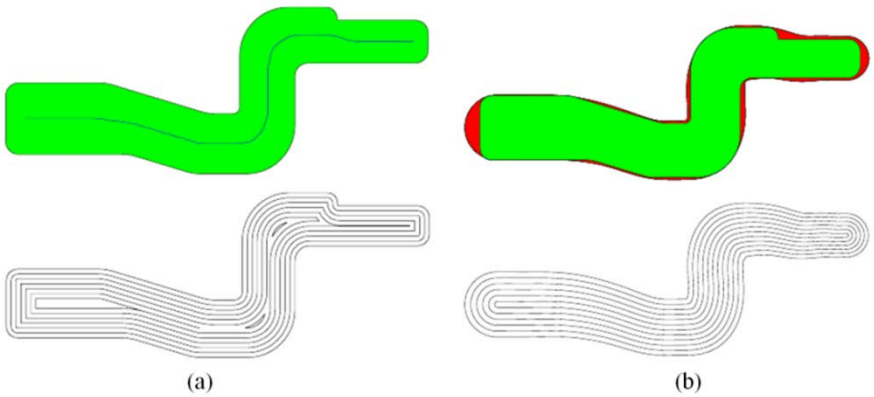

Fig.3 Illustration of path generated from MAT. (a) up: original geometry (green region) and the MAT of the geometry (black line); down: contour path patterns with gaps in middle are clearly seen; (b) up: red region are deposition of excessive materials; down: the MAT path patterns without gaps [28].

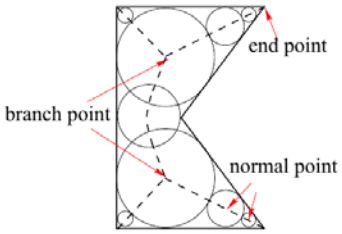

Fig.4 The medial axis transformation (MAT) of an example shape. The dash lines represent the medial axis [28].

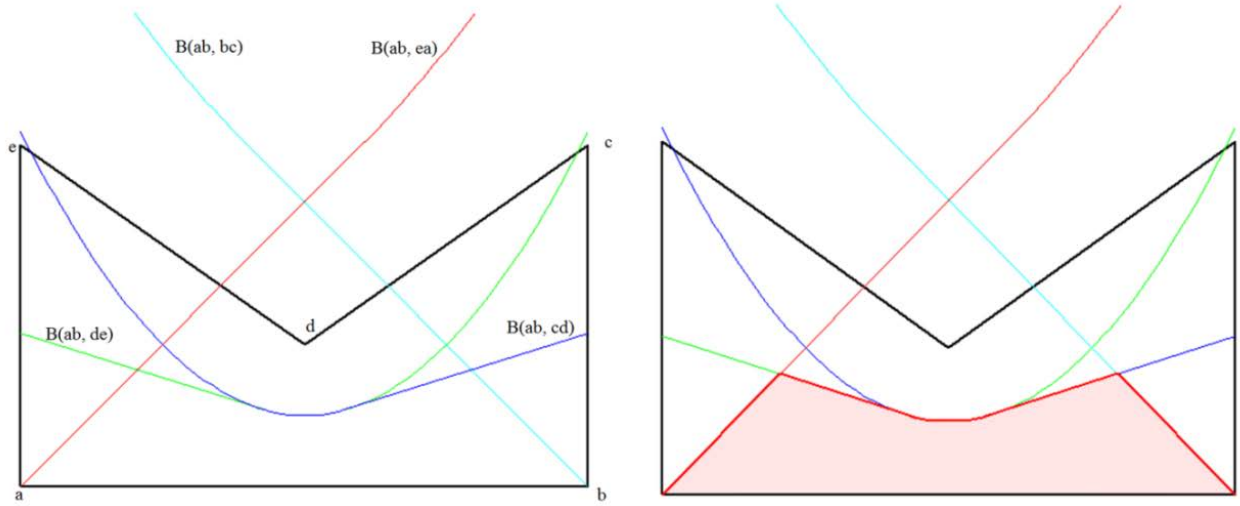

Fig.5 Computation of the bisector lines for pairs of line segments. Black lines represent the boundary of the geometry. Coloured lines represent the bisector lines. Bold red line in (b) represents the MAT corresponding to the boundary *ab*. Pink area is the region in which all points are closet to its associated boundary *ab*.

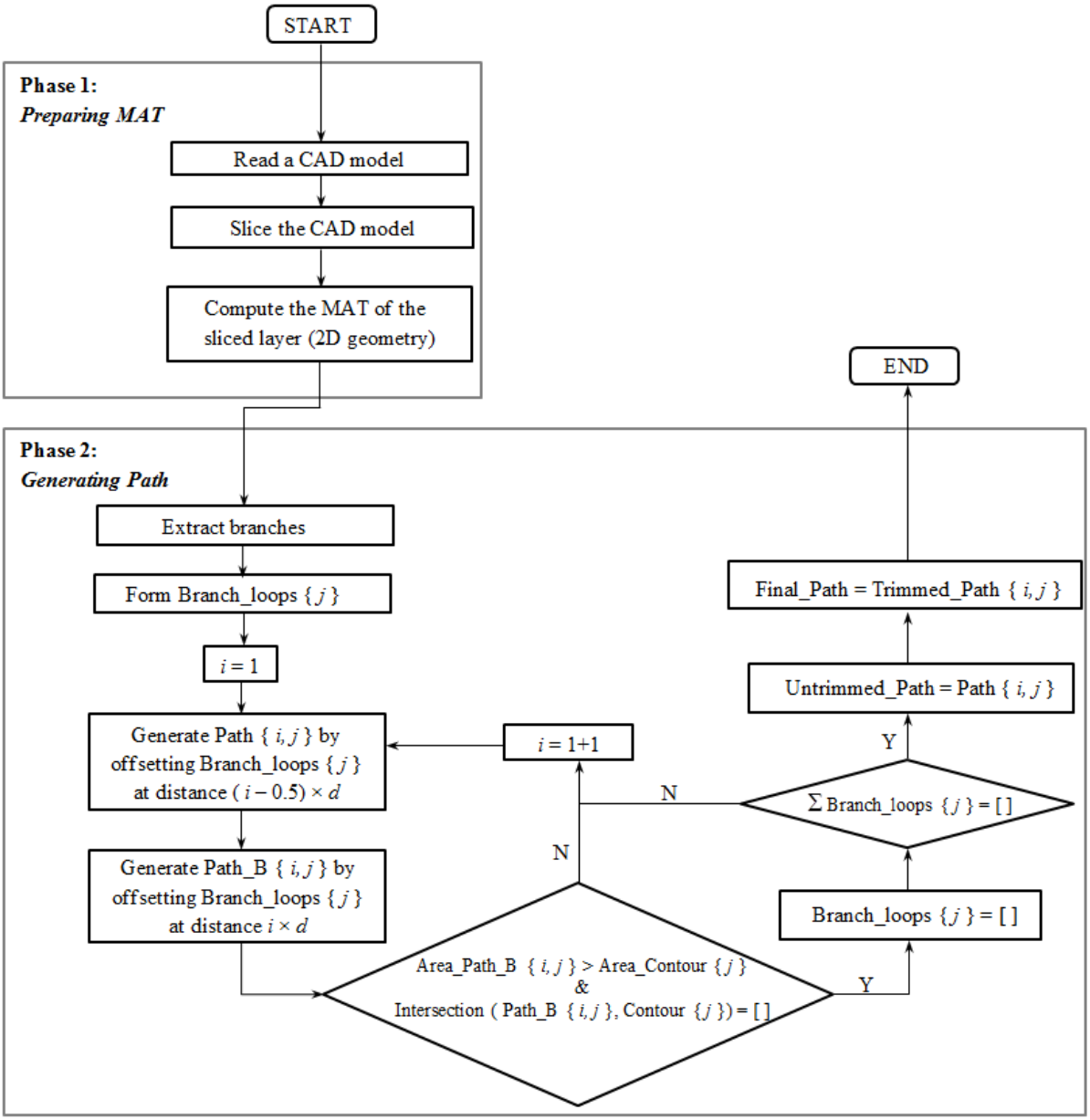

Fig.6 Flowchart of the developed approach for generating path from MAT

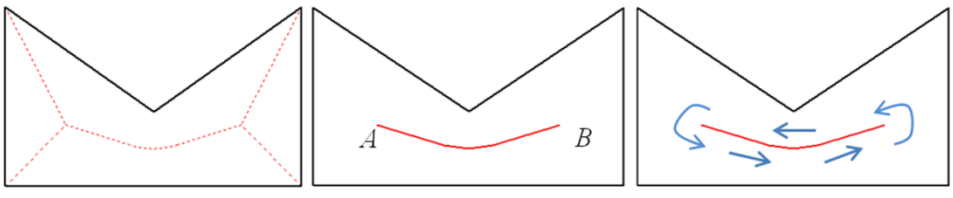

(a) (b) (c)

Fig.7 Example of the shape with single branch and one branch loop. (a) Computed MAT as represented by dotted lines; (b) Single branch from point A to point B as described by red lines; and (c) Formed one branch loop along counter-clockwise direction.

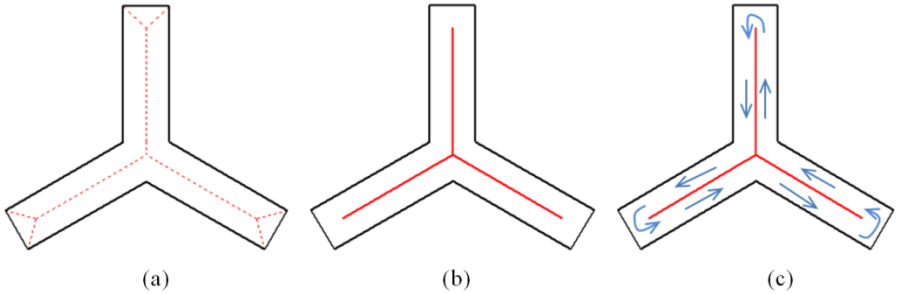

Fig.8 Example of the shape with multiple branches but one branch loop. (a) Computed MAT as represented by dotted lines; (b) Multiple branches as described by red lines; and (c) Formed one branch loop along counter-clockwise direction.

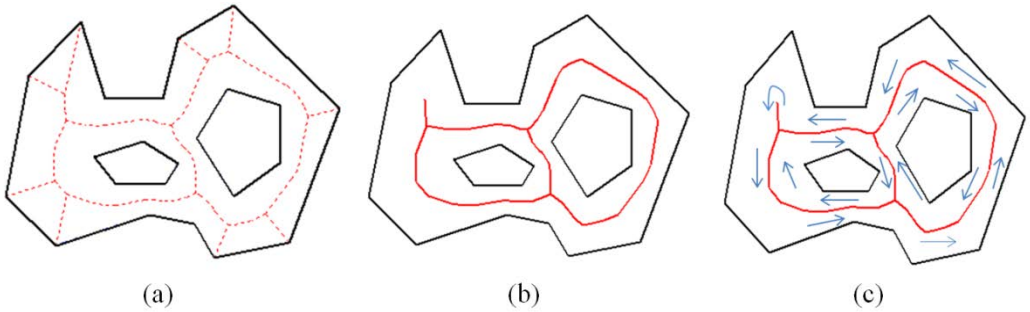

Fig.9 Example of the shape with two holes. (a) Computed MAT as represented by dotted lines; (b) Multiple branches as described by red lines; and (c) Formed one branch loop along counter-clockwise direction and other two branch loops inside along clockwise.

```
UntrimmedPath: 5x3 cell =

    [50x9 double]    [26x9 double]    [32x9 double]
    [44x9 double]    [25x9 double]    [26x9 double]
    [36x9 double]    [13x9 double]    [16x9 double]
    [33x9 double]                []               []
    [30x9 double]                []               []
```

Fig.10 The cell structures of untrimmed paths in the program

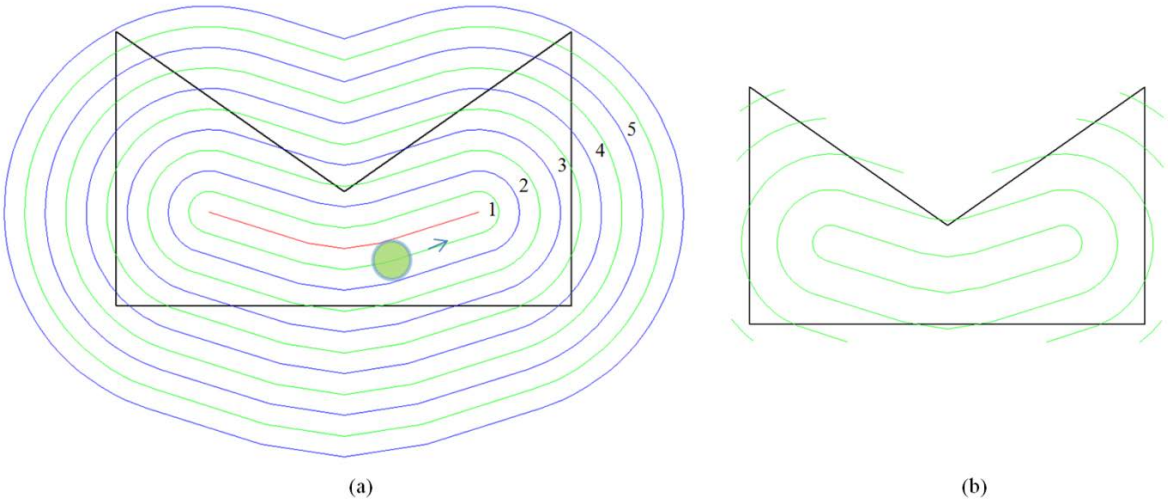

Fig. 11 (a) Untrimmed paths for the simple shape. Black lines represent the boundary of the given geometry. Red lines represent the MAT. Green lines stand for the generated untrimmed paths, and blue lines represent the outside of each untrimmed path. (b) Trimmed paths.

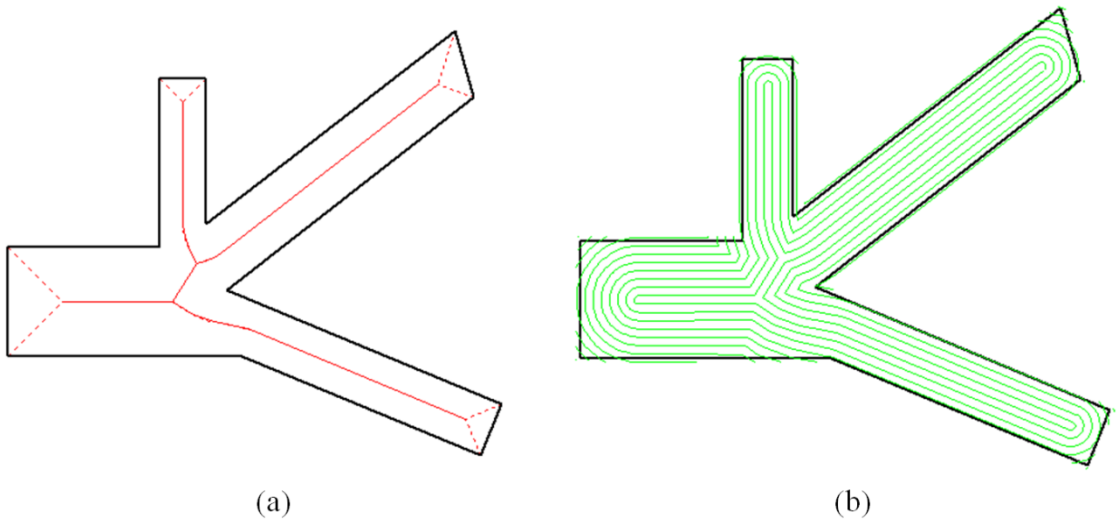

Fig. 12 Geometry 1, solid structure with multiple branches. (a) Geometry is represented by black lines, MAT represented by dotted red lines, and red solid lines stand for branches. (b) Generated trimmed path.

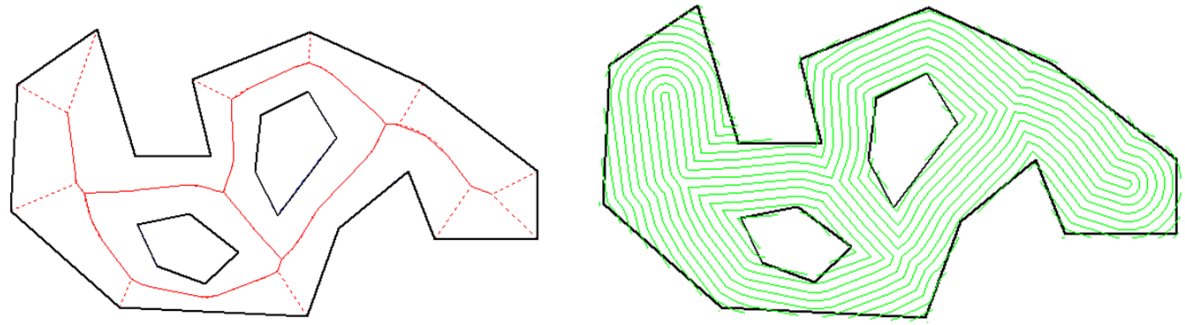

(a) (b)

Fig. 13 Geometry 2, solid structure with holes. (a) Geometry is represented by black lines, MAT represented by dotted red lines, and red solid lines stand for branches. (b) Generated trimmed path.

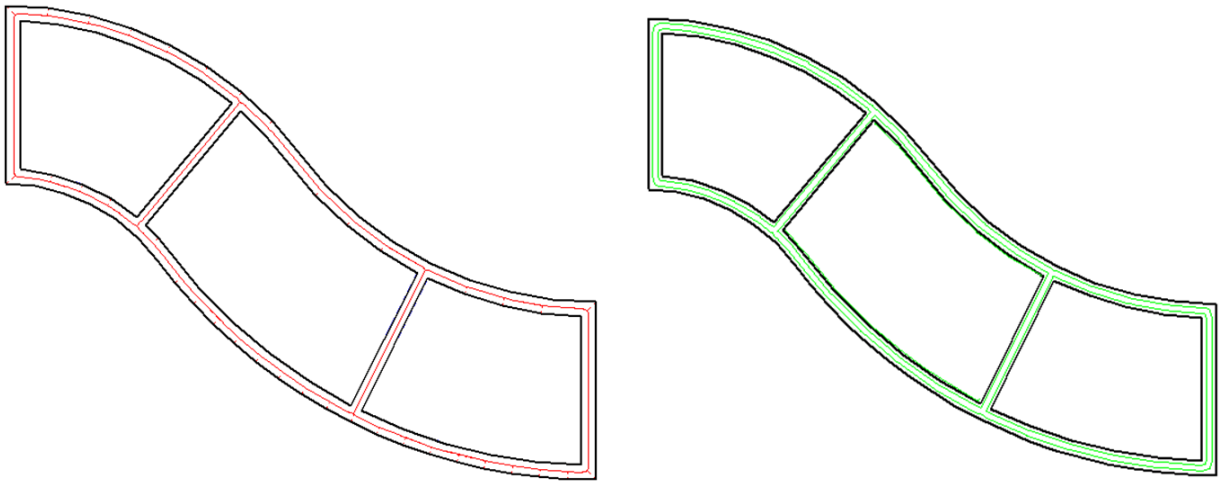

(a) (b)

Fig. 14 Geometry 3, thin-walled curved structure. (a) Geometry is represented by black lines, MAT represented by dotted red lines, and red solid lines stand for branches. (b) Generated trimmed path.

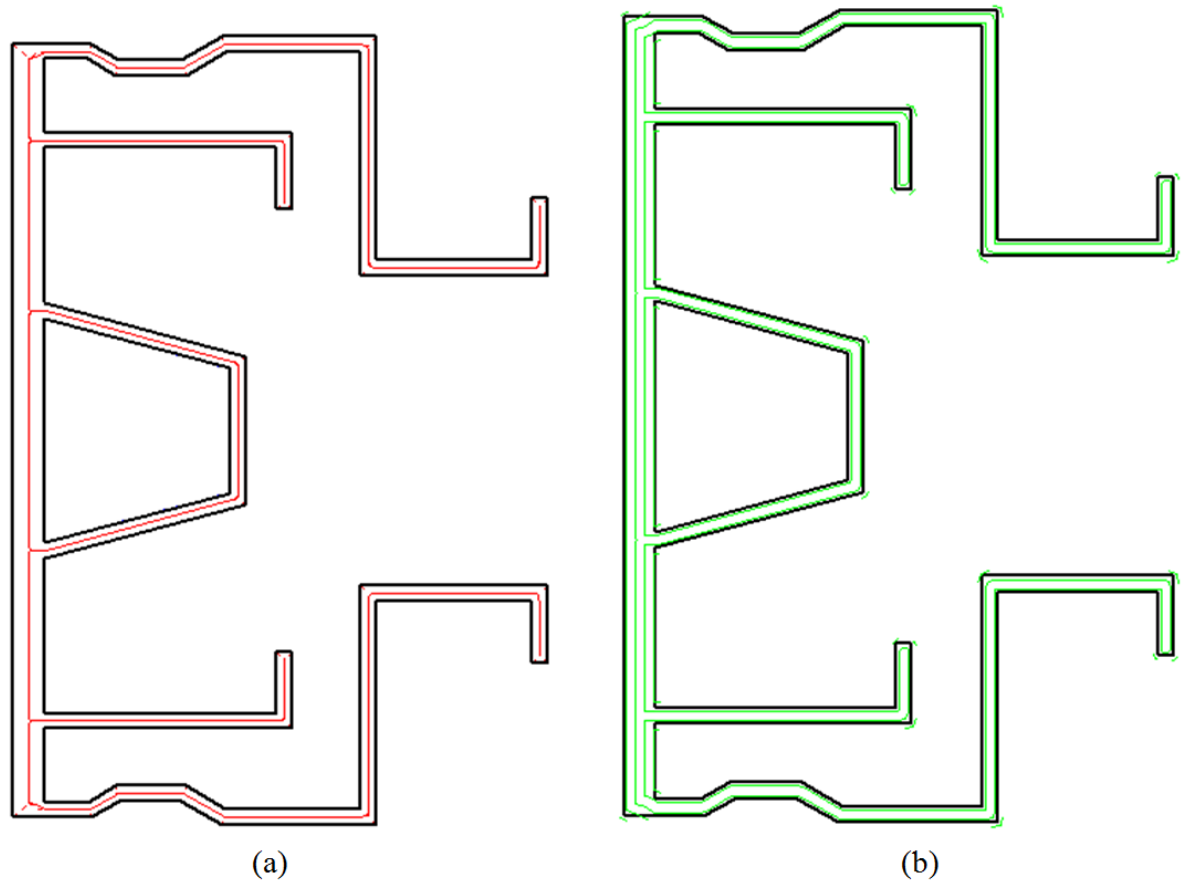

Fig. 15 Geometry 4, thin-walled complex structure. (a) Geometry is represented by black lines, MAT represented by dotted red lines, and red solid lines stand for branches. (b) Generated trimmed path.

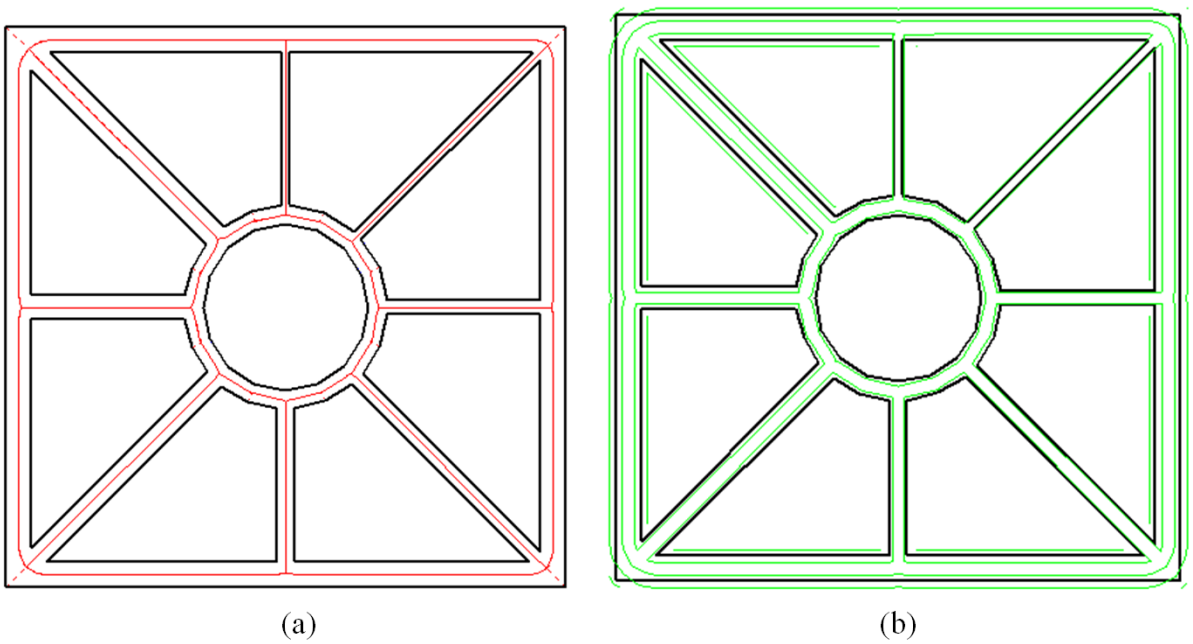

Fig. 16 Geometry 5, thin-walled structure with varied characteristic thicknesses. (a) Geometry is represented by black lines, MAT represented by dotted red lines, and red solid lines stand for branches. (b) Generated trimmed path.

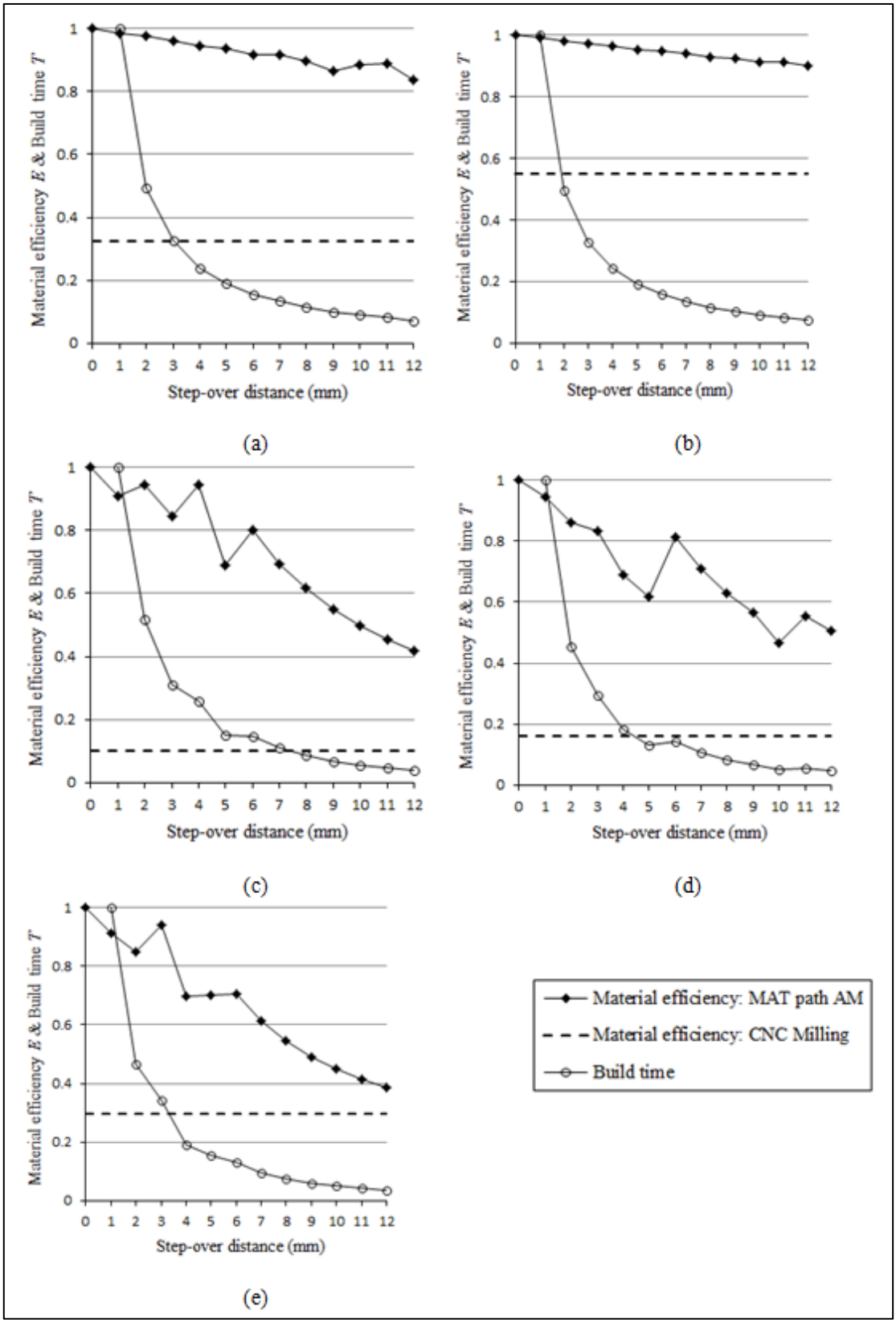

Fig. 17 Material efficiency & non-dimensional build time vs. step-over distance. (a) Geometry 1. (b) Geometry 2. (c) Geometry 3. (d) Geometry 4. (e) Geometry 5.

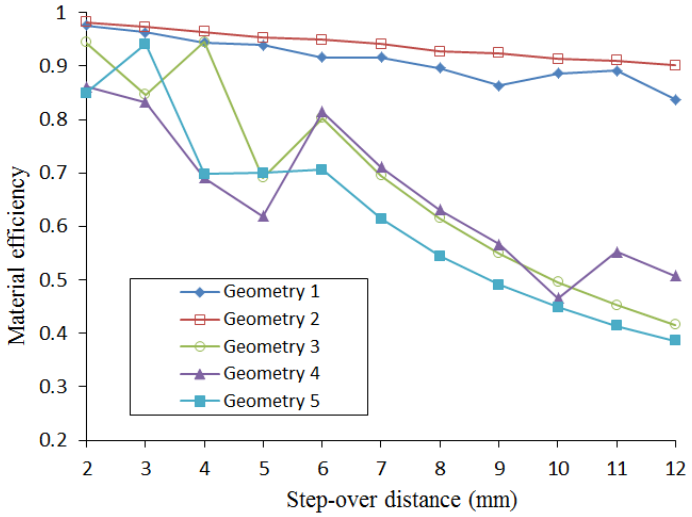

Fig. 18 Material efficiency vs. step-over distance for five geometries in WAAM system

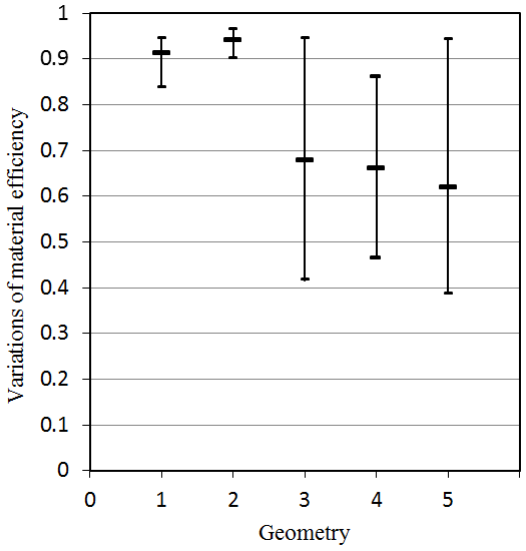

Fig. 19 Variations for material efficiency in wire-feed AM for Geometry 1, 2, 3, 4, and 5.

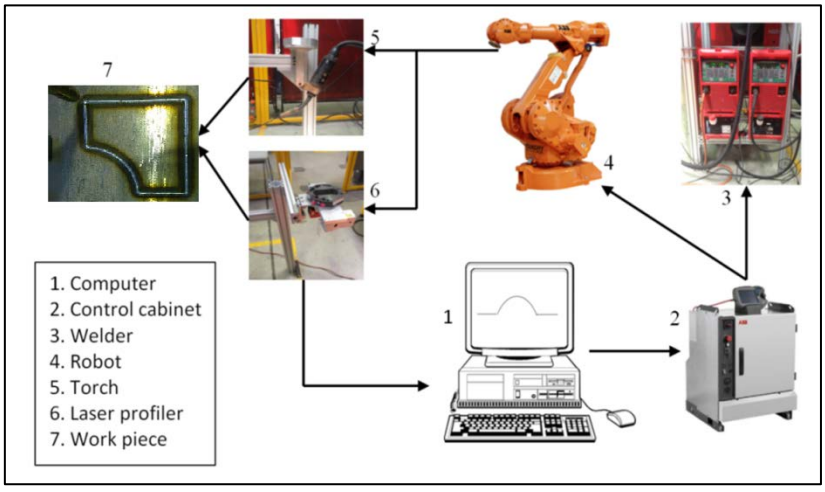

Fig. 20 Schematic diagram of the experimental WAAM system

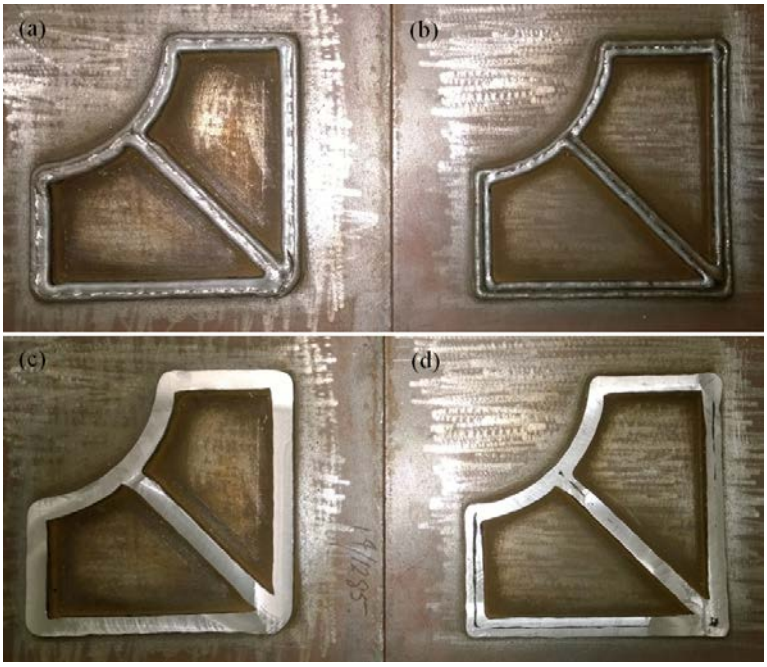

Fig. 21 Experimental comparison of layers produced by the proposed MAT path patterns and the traditional contour path patterns. (a) layers produced by the proposed MAT path patterns. (b) layers produced by the traditional contour path patterns. (c) finished surface of the layers produced by the proposed path patterns. (d) finished surface of the layers produced by the traditional contour path patterns.

Table 1 A brief summary of AM tool-path generation methods.

References	Tool-path pattern	Examples
[13]	Raster	
[14, 15]	Zigzag	
[16-18]	Contour	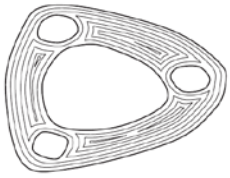
[19, 20]	Spiral	
[21-24]	Continuous	
[25, 26]	Hybrid	

Table 2 Basic information for five case study geometries.

No. Geometry	1	2	3	4	5
Area of enveloped box (× 10^4 mm^2)	28.64	31.06	12.74	17.52	4.84
Area of geometry (× 10^4 mm^2)	9.25	17.06	1.29	2.78	1.44
Volume ratio (%)	32.3	54.9	10.1	15.9	29.8